Rethinking transport
27–30 April 2020

TRA 2020 HELSINKI

Proceedings of 8th Transport Research Arena TRA 2020, April 27-30, 2020, Helsinki, Finland

Modelling and Simulation of Bicycle Dynamics

Murad Shoman[a]*, Hocine Imine[a]

[a]*Université Paris-Est, LEPSIS, IFSTTAR, 14-20 Boulevard Newton, 77420 Champs sur Marne, France*

Abstract

In this paper the authors present an experimental validation of the bicycle simulator developed by two IFSTTAR laboratories: LEPSIS and LPC. In the first part, we focus on improving the dynamics of the bicycle model and simulate the effects of road geometry and surface characteristics such as radius of curvature, road adhesion and unevenness of road profile. In order to verify the accuracy of the developed model, experimental results are shown. For future work, the authors will study the effect of these characteristics on user behaviour to improve the safety and stability of bicycles, particularly in bad weather conditions.

Keywords: Bicycle Modeling, Bicycle Simulator, Simulation, Dynamics, Road characteristics.

* Corresponding author. Tel.: +33 01 81668564;
E-mail address: murad.shoman@ifsttar.fr

1. Introduction

The use of simulators of conduct seems to be an interesting alternative for responding to several challenges such as learning to drive, awareness of risks, road safety, etc. (for example, Babu et al. (2011)), Pieroni et al. (2016) and Ghasemi et al. (2019)). Analysing the cyclist as the centre of this modelling will provide important data on how to improve the quality of modelling as well as understanding the cyclist's behaviour.

Two categories of simulators can be distinguished: motionless simulators and mobile-based simulators. The first is built around a screen providing visual feedback, while the latter provides, in addition to visual information, indices of movements consistent with those of a real vehicle (Nehaoua et al. (2008)). It has been recognized that often a mobile platform, if well controlled, can significantly improve the realism of the simulator of conduct; a good example for this type of simulators is the KAIST bicycle simulator (Kwon et al. (2001) and (2002)) which is consisting of a motion generation system of 6 linear actuators, upper and lower platforms and equipped with an electric Stewart platform on which a bike frame is fixed to provide 6-dof to the handlebar and rear wheel.

There are two main approaches to construct a vehicle mathematical model: The methods of theoretical physics such as Lagrange or Euler are used in order to produce an exact model. The other approach attempts to model the vehicle as simply as possible with little computing-time (Kiencken and Nielsen (2000)). Owczarkowski et al. (2016) used the detailed nonlinear Whipple scientific description to analyse the bicycle mathematical model in which the control law is solved by LQR algorithm. Another bicycle mathematical model was presented by (Qichang He et al. (2005)). The model inhering an interactive bicycle simulator resembling the Korea KAIST bicycle simulator in hardware and two slightly coupled sub-models, namely, the stability sub-model and vibration sub-model. The motion equations were developed based on the Lagrange's equation, and also the Runge–Kutta method was applied to make numerical simulation. Simplifying calculation of the bicycle kinetic energy, the bicycle system is divided into two separate parts; rear and front.

Accordingly, the authors used the classical single-track model, which gives good results for non-critical cycling situations. The developed model will be applied to IFSTTAR bicycle simulator, as well as on an instrumented bicycle in the subsequent work.

Based on the anticipated use of the bicycle simulator, LEPSIS researchers have established a list of features to ensure and constraints to meet these elements (Caro et al. (2015) and Caro & Bernardi (2015)) together with a state of the art on the bicycle simulators which allow to make the technical choices prior to building the simulator. The authors consider the bicycle simulator as a control system in order to obtain the necessary actions to ensure the vehicle's path, such as handlebar angles, pressure on the pedal, etc. The bicycle simulator characteristics make it possible to carry out studies of certain number of situations but does not make it possible to answer all the needs. After the development of the simulator its usability with populations of confirmed cyclists and non-cyclists will be studied. This tool can now be used in studies that require observing the behaviour of cyclists in safe and controllable conditions and measuring the observable variables.

The paper is organised as following, the second part is devoted to bicycle modelling. In the third part, validation results of the model are shown. The fourth part is to present the first experimental results of a developed model of the bicycle simulator. Finally, a conclusion part with some perspectives are presented.

2. Bycile modeling

The bicycle simulator of IFSTTAR shown in the figure 1, has one degree of freedom (steering angle) and is equipped with two force feedback devices: one providing haptic feedback in the handlebars and the other dedicated to the rear wheel. The speed of the rear wheel, the angular position of the handlebar, and the gear are measured and logged. Force feedback is applied to the rear wheel using a cylinder in contact with the wheel.

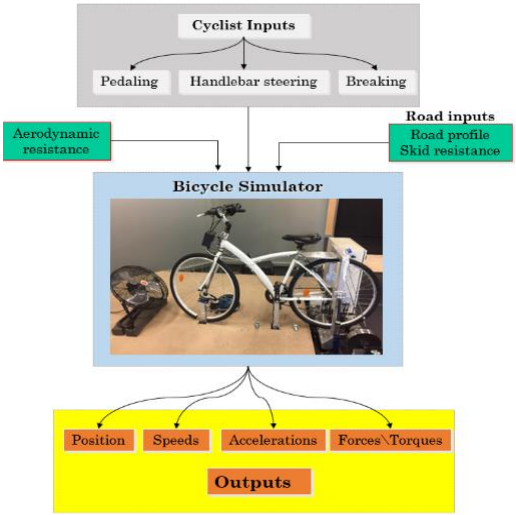

Figure 1. The bicycle model of IFSTTAR

The new model added the following features to the old one developed by Car and al (2015):

- The bicycle model has been developed more and is detailed.
- The vertical model was developed considering the road profile, the vertical displacement of the wheels' centre of gravity, the static normal force and the normal force according to the vertical stiffness of the bicycle.
- The road adhesion was considered when building the longitudinal model of the bicycle wheels.
- The lateral model considers the effect of the side slip angle and the lateral stiffness of the bicycle wheels.

A scheme for different interactive parts of the model is presented in Fig. 2. Each part will be detailed in the next sections.

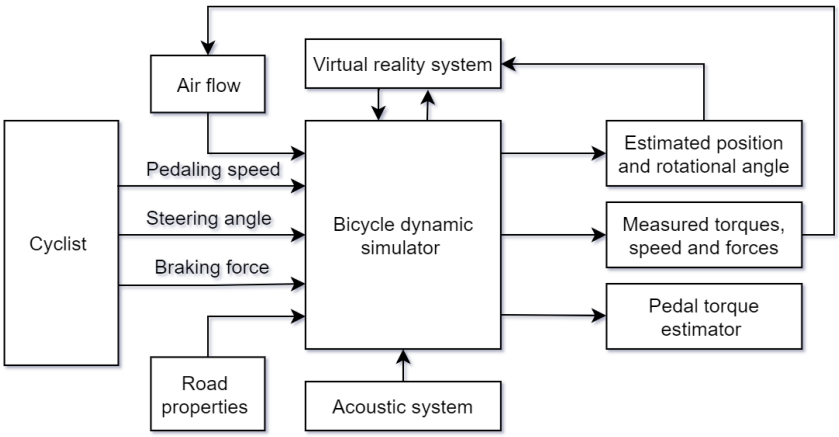

Figure 2. Operating flow of the bicycle simulator

The mechanical torque of the force feedback is related to the speed as indicated by the following equation:

$$F = 10 + k.V \quad (1)$$

Where F is the resisting force applied to the pneumatic in N. V is the tangential speed of the pneumatic in m/s (i.e., the speed at which the bicycle should move). The constant k can be manipulated.

2.1. Vertical modeling

The tyres of the front and rear wheels are modelled by a spring with coefficient k_F and k_R. The wheel mass is given by m_F *and* m_R. At the tire contact, the road profile, the skid resistance, and the radius of curvature are considered inputs of the system. The road profile is represented by the variable u. The pitch angle of the bicycle is neglected. Fig. 3 shows the vertical model of the bicycle.

The vertical acceleration values of the wheels are obtained using the following equations:

$$\ddot{z}_F = \frac{-\mathrm{k}_F z_F + \mathrm{k}_F \mathrm{u}_\mathrm{F}}{m_F} \quad (2)$$

$$\ddot{z}_R = \frac{-\mathrm{k}_R z_R + \mathrm{k}_R u_R}{m_R} \quad (3)$$

Where m_F *and* m_R are the masses of the front and rear wheel, k_F and k_R are the front and rear tyres vertical stiffness, z_F *and* z_R are the vertical displacement of the COG of the front and rear wheel respectively, u_F and u_R are respectively the front and rear value of road profile. To obtain the vertical displacement z_R we integrate twice this acceleration.

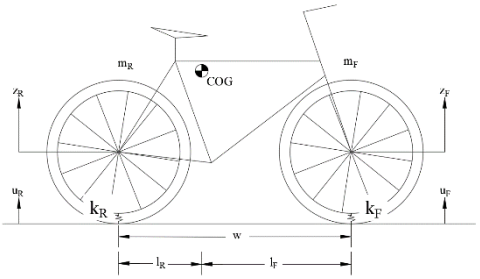

Figure 3. Side view of the bicycle model.

The normal forces F_{nF} *and* F_{NR} acting on the wheels are calculated as following:

$$F_{nF} = F_{cF} + k_F(u_F - z_F) \quad (4)$$

$$F_R = F_{cR} + k_R(u_R - z_R) \quad (5)$$

Where F_{cF} *and* F_{cR} are the static force due to the static mass of the vehicle.

In this paper, the force generated by damping effects is neglected, in comparison with spring forces $k_i(u_i - z_i)$.

2.2. Lateral modeling

In order to calculate the wheel forces, it is necessary to know wheel slip, tire side slip angle and friction coefficients, as these are inputs for the force equations. For the tire side slip angle calculation, the wheel caster has to be taken into consideration and the curve radii of the individual wheels, see equations (6 to 11).

$$\alpha_F = -\beta + \delta_W - \frac{l_F \cdot \dot{\psi}}{v_{COG}} \quad (6)$$

$$\alpha_R = -\beta + \frac{l_R \cdot \dot{\psi}}{v_{COG}} \quad (7)$$

Where α_F *and* α_R are the side slip angles for the front and rear wheel respectively, β is vehicle body side slip angle, δ_W is the steering angle of the handlebar, l_F *and* l_R are distances from COG to front and rear axles,v_{COG} is the Centre of Gravity velocity, $\dot{\psi}$ is the yaw rate calculated using equation (7)

$$\dot{\psi} = \frac{V}{R} \quad (8)$$

Where V is the bicycle speed and R is the radius of curvature calculated using following equation (9).

$$R = \frac{l_f + l_r}{\sin \delta_s} \quad (9)$$

Where δ_s is the steering angle.

After calculation of the different parameters, it is possible to calculate the lateral force for both the front and rear wheel using the following equations.

$$F_{yF} = \alpha_F \times C_y \quad (10)$$

Where F_{yF} *and* F_{yR} are the lateral forces of the front and rear wheel respectively and C_Y is the tyre lateral stiffness.

2.3. Longitudinal modeling

The Longitudinal frictional forces of the front and rear wheels can be calculated from the adhesion co-efficient using Equation (12) and (13). This provides the frictional forces in the direction of the wheel ground contact velocity.

$$F_{xF} = \mu \times F_{zF} \times \cos\ \alpha_F \tag{11}$$

$$F_{xR} = \mu \times F_{zR} \times cos\ \alpha_R \tag{12}$$

Where $F_{xF}\ and\ F_{xR}$ are the longitudinal forces for the front and rear wheel respectively, μ is the adhesion coefficient of the surface and $F_{zF}\ and\ F_{zR}$ are the vertical forces applied on the front and rear wheels. In the next section, some validation results will be presented in order to show the accuracy of the presented model.

3. Validation results

Several tests and scenarios have been realized at various speeds with the bicycle simulator. Selected results of the vertical displacement and forces, side slip angle, lateral forces and longitudinal forces are presented in the following. The dynamic parameters and the static vertical forces are stated from the literature (Moore et al. (2009) and (2010) Bulsink et al. (2015)). The values of the static front and rear vertical forces (which were calculated according to the combined mass of the bicycle and rider by applying the equilibrium equations with known COG) are 230 and 630 N, respectively.

3.1. Vertical displacement and force

The longitudinal road profile, which has been measured in a previous experiment conducted by IFSTTAR) is used as an input signal for the Simulink model (see Fig.4). A close up on the time interval of [10, 15] s is given on the right side of the figure. The vertical displacement with a close up on the time interval of [10, 15] s to the right shown in Fig. 5 was estimated using equations. (2) and (3). Despite the double filtering effect caused by integrating two times, the two signals indicate the correct behaviour of the model.

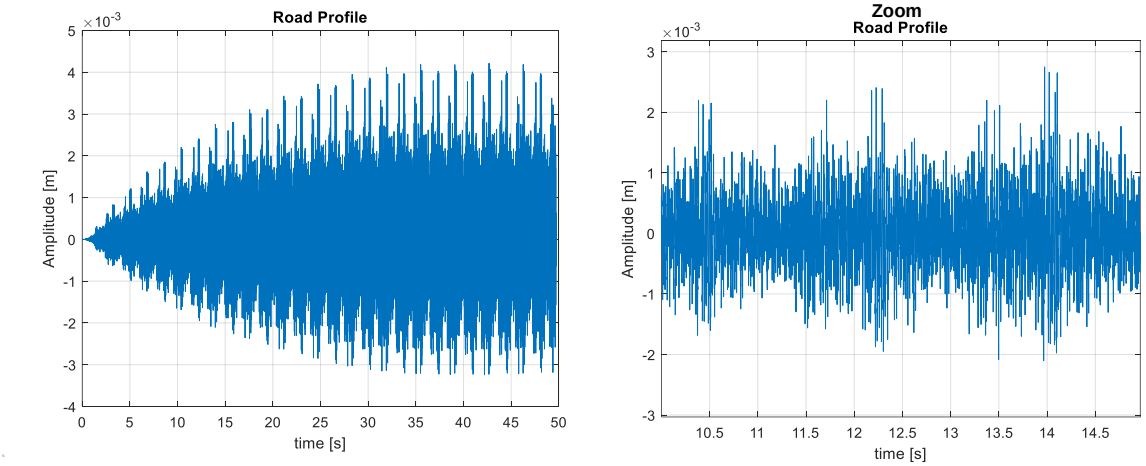

Figure 4. Road profile input.

In Fig. 6, the vertical forces of the front and rear wheels are presented. The close up on the time interval of [10, 15] s is displayed on the right side of this figure 6. It can be noticed that at the 10.5th, 12.3th, and 14th second, the vertical force increases following the amplitude of the road profile at this time.

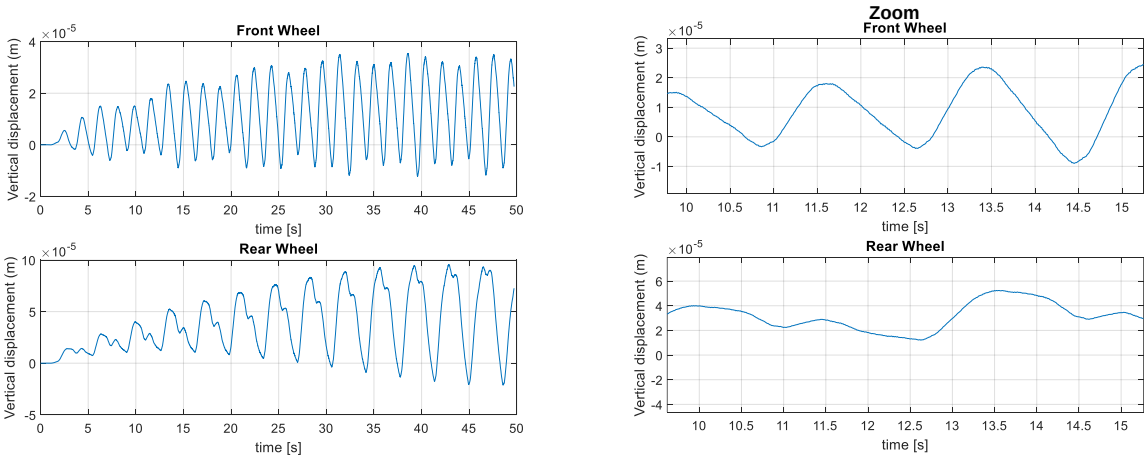

Figure 5. Vertical displacement (z).

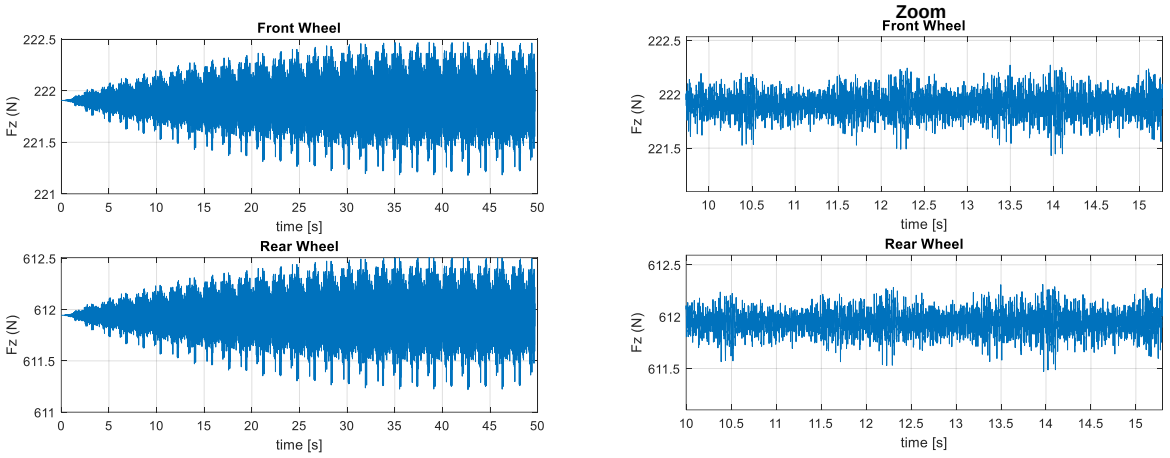

Figure 6. Vertical force.

3.2. Side slip angle and lateral force

The steering angle of the bicycle handlebar during the test (shown in Fig.7) was measured using an incremental encoder connected to the handlebar of the bicycle simulator. The side slip angle shown in Fig. 8 noticeably reflects the angular movement of the handlebar.

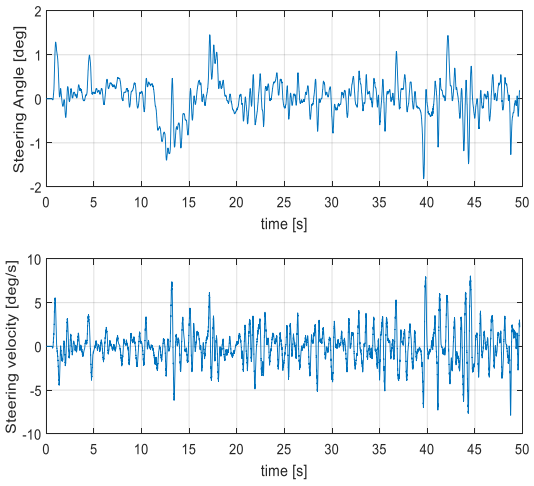

Figure 7. Steering angle and velocity.

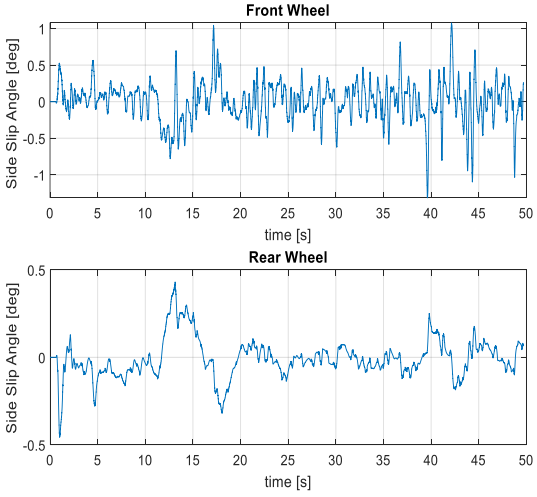

Figure 8. Side slip angle.

The lateral trajectory of the bicycle as shown in Fig. 9 is perceived to be affected by the steering angle. With a closer look at the span between [10,15] s, the effect of high steering angle on the trajectory can be observed.

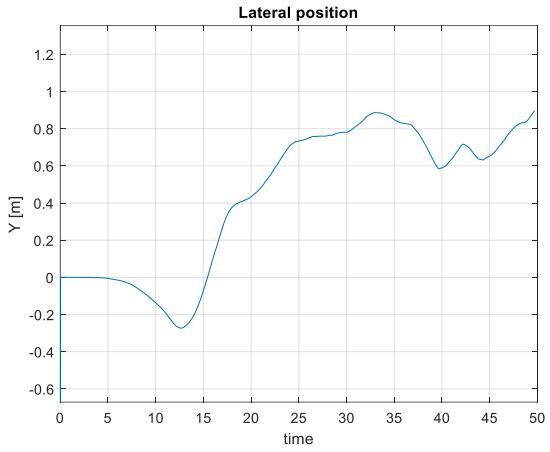

Figure 9. Lateral position.

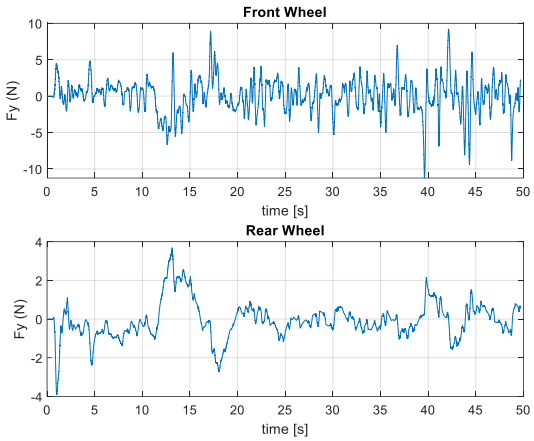

Figure 10. Lateral force.

Fig. 10 shows the lateral force of the front and rear wheels. The graphs show that the increase of the sides slip angle causes an increase in the lateral force, this becomes obvious at 40th and 45th second.

3.3. Longitudinal force

In the simulation several adhesion coefficient representing different surfaces and different weather conditions came to use. The longitudinal force shown in Fig. 12, which was calculated based on the adhesion coefficient (Fig. 11), shows the impact of different adhesion coefficient. While the road surface is dry ($\mu = 0.8$) the longitudinal friction force in high whereas a wet surface ($\mu = 0.2$) results in a low longitudinal friction force.

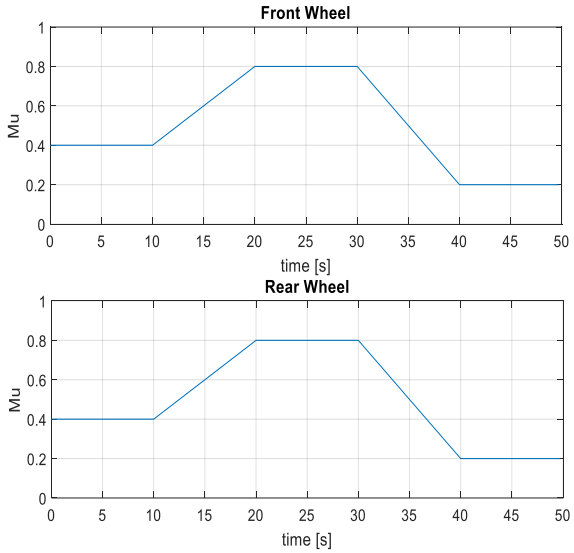

Figure 11. Adhesion coefficient.

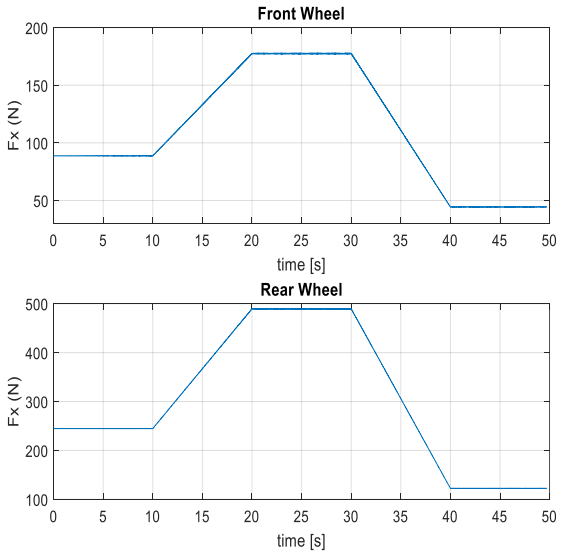

Figure 12. Longitudinal force.

4. Experimentation description

4.1. Experimental setup

The bicycle simulator has been built by placing a real bicycle on a platform (see Fig. 13). The computing environment is constituted by a PC and the software: Matlab, Simulink and Real Time Workshop.

In order to provide more realistic circumstances, the simulator consists of several components:

- 5 visual displays installed in front of the bicycle to provide simulated conditions similar to real-life environment. The visual displays provide a visual angle of 225 degrees in the horizontal direction and 55 degrees in the vertical direction.
- A flywheel attached to the rear wheel simulates inertia equal to 60 kg mass in actual cycling. The simulator is also equipped with an incremental encoder able to increase the inertia up to 85 kg as in actual cycling.
- A fan is placed in front of the bicycle reproducing the airflow felt by cyclists in a real situation. The airflow speed is proportional to the wheel's speed.
- A passive mechanical system allows participants to slightly tilt the bike.

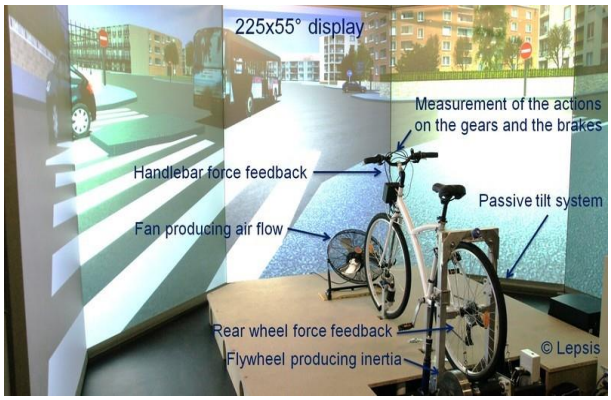

Figure 13. IFSTTAR bicycle simulator.

Ten participants (6 male; mean age=28.17, SD=3.76 and 4 females; mean age=25.25, SD=2.06) took part in this experiment. All had normal or corrected-to-normal vision. The mean cycling experience of the participants was 12.9 years. The average number of cycling kilometers per month was 62. None of them rode a bicycle simulator before.

The experiment took place in a simulated urban environment. The road consists of two sections: the first is a bicycle-bus shared lane, the latter with a separated bicycle lane. The participants took a pre-ride for 2 minutes in order to familiarize themselves with the simulator. After the end of the familiarization, the participants rode the bicycle for 10 minutes. The traffic was generated at the same and opposite directions of the cyclist and buses were passing beside the cyclist from time to time. The participants were asked to maneuver with the simulator using the different features such as: handlebar, pedals, gear and brakes.

4.2. Experimentation results

At the end of the experiment, the participants completed a questionnaire regarding their cycling experience and the impact of the bicycle simulator on their personal status. The questionnaire consists of the NASA Task Load Index (TLX) form (Hart (1986)) which is used to assess the work load and the Simulator Sickness Questionnaire by Kennedy et al. (1993) to evaluate the different symptoms of the bicycle simulator.

The analysis of TLX for the 10 participants shows that the simulator requires a medium physical demand. This is explained by the effort the participants required to do when riding any bicycle since it is an active transport mode. Fig. 14 shows more results about the different aspects of the work load.

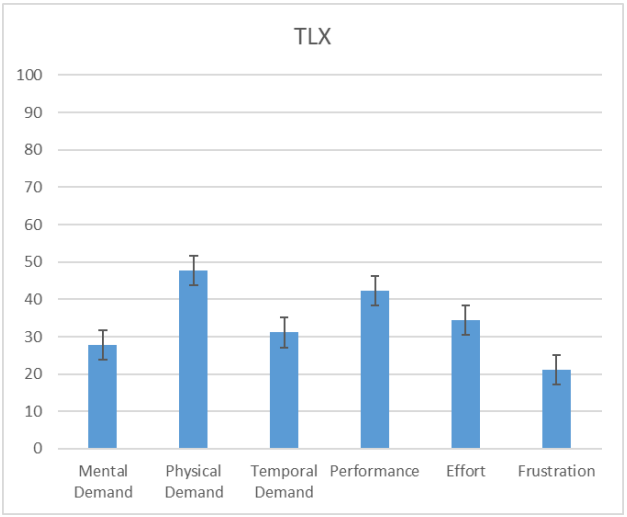

Figure 14. Work load of the bicycle simulator.

The analysis of the simulation sickness questionnaire shows that one participant had the symptoms of simulator sickness. The participant suffered from severe symptoms of eye strain, difficulty focusing, sweating, nausea and dizziness with eyes open. The participant was immediately asked to stop the experiment. 30% of the participants felt a slight general discomfort and 30% experienced a slight sweating increase. For the complete results of the simulator sickness questionnaire see Appendix A.1.

5. Conclusion

This work leads to develop and validate the existing bicycle simulator. By conducting comparative studies between the theoretical and practical aspects, it is possible to verify the reliability of the simulator. The results obtained from experimental studies show the accuracy of the developed model even if some additional works should be done to enhance the bicycle model. The results show that dynamic states of the bicycle model are well estimated. (Estimation of the vertical displacement and side slip angle are presented.). the effect of these inputs on calculation of vertical, lateral and longitudinal forces are observed. The result shows the direct impact of steering angle on the side slip angle estimation which accordingly affect the calculation of the lateral and longitudinal forces, the impact of the vertical displacement is also observed on the vertical forces.

In perspective work a real time estimation of the road adhesion coefficient and wheel slip will be included in the model. In subsequent studies it would be interesting to reproduce these experiments in different scenarios of locations and countries in order to test the developed algorithms on the simulator and on the road. The bicycle simulator enables us to put cyclists in a riding situation and accurately measure their effective behavior, while controlling the variables at play and avoiding the risks associated with a real environment.

Acknowledgements

This works is funded by Marie Skłodowska-Curie actions (H2020 MGA MSCA-ITN) within the SAFERUP project (grant agreement number 765057). The authors gratefully acknowledge their contributions.

References

Babu, SV, Grechkin, TY, Chihak, B., Ziemer, C., Kearney, JK, Cremer, JF, & Plumert, JM (2010). An immersive virtual peer for studying social influences on child cyclists' road-crossing behavior. IEEE Transactions on Visualization and Computer Graphics, 17 (1), 14-25.

Caro, S., & Bernardi, S. (2015). The role of various sensory cues in self-speed perception: a bicycle riding simulator preliminary study. In DSC 2015-Driving simulation conference.

Nehaoua, L. (2008). Conception et réalisation d'une plateforme mécatronique dédiée à la simulation de conduite des véhicules deux-roues motorisés (Doctoral dissertation, Université d'Evry-Val d'Essonne).

Kwon, D. S., Yang, G. H., Lee, C. W., Shin, J. C., Park, Y., Jung, B., ... & Wohn, K. Y. (2001, May). KAIST interactive bicycle simulator. In Proceedings 2001 ICRA. IEEE International Conference on Robotics and Automation (Cat. No. 01CH37164) (Vol. 3, pp. 2313-2318). IEEE.

Kwon, D. S., Yang, G. H., Park, Y., Kim, S., Lee, C. W., Shin, J. C., ... & Lee, D. Y. (2002, October). KAIST interactive bicycle racing simulator: the 2nd version with advanced features. In IEEE/RSJ International Conference on Intelligent Robots and Systems (Vol. 3, pp. 2961-2966). IEEE.

Kiencke, U., & Nielsen, L. (2000). Automotive control systems: for engine, driveline, and vehicle.

Owczarkowski, A., Horla, D., Kozierski, P., & Sadalla, T. (2016). Dynamic modeling and simulation of a bicycle stabilized by LQR control. In 2016 21st International Conference on Methods and Models in Automation and Robotics (MMAR) (pp. 907-911). IEEE.

He, Q., Fan, X., & Ma, D. (2005). Full bicycle dynamic model for interactive bicycle simulator. Journal of Computing and Information Science in Engineering, 5(4), 373-380.

Caro, S., Vienna, F., Chaurand, N., Dang, NT, Bernardi, S., & Ramdani, B. (2015, December). An Îlo simulator for new research.

Ghasemi, N., Imine, H & Simone, A., Lantieri, C., & Vignali, V. (2019). Longitudinal Motion Cueing Effects on Driver Behaviour: A Driving Simulator Study. Advances in Transportation Studies: an international Journal Section B 49.

Pieroni, A., Lantieri, C., Imine, H., & Simone, A. (2016). Light vehicle model for dynamic car simulator. Transport, 31(2), 242-249.

Moore, J. K., Hubbard, M., Kooijman, J. D. G., & Schwab, A. L. (2009, January). A method for estimating physical properties of a combined bicycle and rider. In ASME 2009 international design engineering technical conferences and computers and information in engineering conference (pp. 2011-2020). American Society of Mechanical Engineers.

Moore, J. K., Hubbard, M., Schwab, A. L., & Kooijman, J. D. (2010, October). Accurate measurement of bicycle parameters. In Proceedings, Bicycle and Motorcycle Dynamics 2010 Symposium on the Dynamics and Control of Single-Track Vehicles, 20Ű22 October 2010, Delft, The Netherlands.

Bulsink, V. E., Doria, A., van de Belt, D., & Koopman, B. (2015). The effect of tyre and rider properties on the stability of a bicycle. Advances in mechanical engineering, 7(12), 1687814015622596.

Hart, S. G. (1986). NASA Task load Index (TLX). Volume 1.0; Paper and pencil package.

Kennedy, R.S., Lane, N.E., Berbaum, K.S., & Lilienthal, M.G. (1993). Simulator Sickness Questionnaire: An enhanced method for quantifying simulator sickness. International Journal of Aviation Psychology, 3(3), 203-220.

A.1 Results of the simulator sickness questionnaire